BDPA-Nitroxide Biradicals Tailored for Efficient Dynamic Nuclear Polarization Enhanced Solid-State NMR at Magnetic Fields up to 21.1

(Article begins on next page)

07 May 2024

9-25-2018

BDPA-Nitroxide Biradicals Tailored for Efficient Dynamic Nuclear Polarization Enhanced Solid-State NMR at Magnetic Fields up to 21.1 T

Dorothea Wisser
Université de Lyon

Ganesan Karthikeyan
Aix-Marseille Université

Alicia Lund
Université de Lyon

Gilles Casano
Aix-Marseille Université

Hakim Karoui
Aix-Marseille Université

Follow this and additional works at: https://lib.dr.iastate.edu/chem_pubs

See next page for additional authors

Part of the Materials Chemistry Commons

The complete bibliographic information for this item can be found at https://lib.dr.iastate.edu/chem_pubs/1071. For information on how to cite this item, please visit http://lib.dr.iastate.edu/howtocite.html.

BDPA-Nitroxide Biradicals Tailored for Efficient Dynamic Nuclear Polarization Enhanced Solid-State NMR at Magnetic Fields up to 21.1 T

Abstract

Dynamic Nuclear Polarization (DNP) solid-state NMR has developed into an invaluable tool for the investigation of a wide range of materials. However, the sensitivity gain achieved with many polarizing agents suffers from an unfavorable field and Magic Angle Spinning (MAS) frequency dependence. We present a series of new hybrid biradicals, soluble in organic solvents, that consist of an isotropic narrow EPR line radical, BDPA, tethered to a broad line nitroxide. By tuning the distance between the two electrons and the substituents at the nitroxide moiety, correlations between the electron-electron interactions and the electronic spin relaxation times on one hand, and the DNP enhancement factors on the other hand are established. The best radical in this series has a short methylene linker and bears bulky phenyl spirocyclohexyl ligands. In a 1.3 mm prototype DNP probe, it yields enhancements of up to 185 at 18.8 T (800 MHz 1H resonance frequency) and 40 kHz MAS. We show that this radical gives enhancement factors of over 60 in 3.2 mm sapphire rotors at both 18.8 and 21.1 T (900 MHz 1H resonance frequency), the highest magnetic field available today for DNP. The effect of the rotor size and of the microwave irradiation inside the MAS rotor is discussed. Finally, we demonstrate the potential of this new series of polarizing agents by recording high field 27Al and 29Si DNP Surface Enhanced NMR spectra (DNP SENS) of amorphous aluminosilicates and 17O NMR on silica nanoparticles.

Disciplines

Chemistry | Materials Chemistry

Authors

Dorothea Wisser, Ganesan Karthikeyan, Alicia Lund, Gilles Casano, Hakim Karoui, Maxim Yulikov, Georges Menzildjian, Arthur C. Pinon, Armin Purea, Frank Engelke, Sachin R. Chaudhari, Dominik Kubicki, Aaron Rossini, Ilia B. Moroz, David Gajan, Christophe Copéret, Gunnar Jeschke, Moreno Lelli, Lyndon Emsley, Anne Lesage, and Olivier Ouari

BDPA-Nitroxide Biradicals Tailored for Efficient Dynamic Nuclear Polarization Enhanced Solid-State NMR at Magnetic Fields up to 21.1 T

Dorothea Wisser,[a] Ganesan Karthikeyan,[b] Alicia Lund,[a] Gilles Casano,[b] Hakim Karoui[b] Maxim Yulikov,[c] Georges Menzildjian,[a] Arthur C. Pinon,[d] Armin Purea,[e] Frank Engelke,[e] Sachin R. Chaudhari,[a]† Dominik Kubicki,[d] Aaron J. Rossini,[d]$ Ilia B. Moroz,[c] David Gajan,[a] Christophe Copéret,[c] Gunnar Jeschke,[c] Moreno Lelli,[f,g]* Lyndon Emsley,[d]* Anne Lesage,[a]* Olivier Ouari[b]*

[a] Institut de Sciences Analytiques, Centre de RMN à Très Hauts Champs, Université de Lyon (CNRS/ENS Lyon/UCB Lyon 1), 69100 Villeurbanne, France

[b] AixMarseille Univ, CNRS, ICR, 13013 Marseille, France

[c] Department of Chemistry and Applied Biosciences, Eidgenössische Technische Hochschule Zürich, CH-8093 Zürich, Switzerland

[d] Institut des Sciences et Ingénierie Chimiques, Ecole Polytechnique Fédérale de Lausanne (EPFL), CH-1015 Lausanne, Switzerland

[e] Bruker Biospin, 76287 Rheinstetten, Germany

[f] Department of Chemistry "Ugo Schiff", University of Florence, Via della Lastruccia 3, 50019 Sesto Fiorentino (FI), Italy.

[g] Magnetic Resonance Center (CERM), University of Florence, Via L. Sacconi 6, 50019 Sesto Fiorentino (FI), Italy.

Dynamic Nuclear Polarization • Nuclear Magnetic Resonance • polarizing agents • Cross Effect • biradicals

ABSTRACT: Dynamic Nuclear Polarization (DNP) solid-state NMR has developed into an invaluable tool for the investigation of a wide range of materials. However, the sensitivity gain achieved with many polarizing agents suffers from an unfavorable field and Magic Angle Spinning (MAS) frequency dependence. We present a series of new hybrid biradicals, soluble in organic solvents, that consist of an isotropic narrow EPR line radical, BDPA, tethered to a broad line nitroxide. By tuning the distance between the two electrons and the substituents at the nitroxide moiety, correlations between the electron-electron interactions and the electronic spin relaxation times on one hand, and the DNP enhancement factors on the other hand are established. The best radical in this series has a short methylene linker and bears bulky phenyl spirocyclohexyl ligands. In a 1.3 mm prototype DNP probe, it yields enhancements of up to 185 at 18.8 T (800 MHz ^{1}H resonance frequency) and 40 kHz MAS. We show that this radical gives enhancement factors of over 60 in 3.2 mm sapphire rotors at both 18.8 and 21.1 T (900 MHz ^{1}H resonance frequency), the highest magnetic field available today for DNP. The effect of the rotor size and of the microwave irradiation inside the MAS rotor is discussed. Finally, we demonstrate the potential of this new series of polarizing agents by recording high field ^{27}Al and ^{29}Si DNP Surface Enhanced NMR spectra (DNP SENS) of amorphous aluminosilicates and ^{17}O NMR on silica nanoparticles.

1. INTRODUCTION

Dynamic Nuclear Polarization (DNP) is one of the most promising approaches to overcome the intrinsic sensitivity limitations of solid-state NMR, opening new possibilities and applications in materials and life sciences.[1-7] The recent advances result from significant developments in DNP instrumentation, introduction of new methodological concepts, and the design of ever more efficient polarization sources. Today, the most commonly used polarizing agents for solid-state DNP NMR are dinitroxides that exploit the Cross Effect (CE) polarization transfer mechanism.[1-2, 8] The molecular structures, *i.e.* the relative orientation of the nitroxide *g*-tensors, the distance between the two unpaired electrons, the nature of the groups decorating the nitroxide moieties or their deuteration level, have been extensively studied and rationally optimized in the past few years.[9-15] This has led to the introduction of highly efficient radicals at intermediate fields (9.4 T, 400 MHz ^{1}H resonance frequency) such as TEKPol[12], AMUPol,[11] SPIROPOL,[16] Py-PolPEG$_2$OH[17] or bcTol,[18] that give signal enhancements of up to 300 (at 9.4 T and ~100 K) in a broad range of solvent formulations,[11, 13, 19] or more if sample formulations are optimized, for instance by adding dielectric particles.[20]

High magnetic fields (>10 T) and fast Magic Angle Spinning (MAS) frequencies (>10 kHz) are often prerequisites for advanced atomic-scale characterization by solid-state NMR, as they both contribute to increased sensitivity and spectral resolution. In these regimes, dinitroxides suffer however from two drawbacks. First, as their EPR line width increases linearly with the external field (B_0), the efficiency of the CE mechanism is expected to scale at least with $1/B_0$.[8] Recent theoretical work on CE DNP enhancements under MAS predicts a field dependence varying between $1/B_0$ and $1/B_0^3$.[21-23] Thus, when doubling the magnetic field from 9.4 T to 18.8 T, the ^{1}H enhancement ε_H of frozen solutions typically drops from 250 to about 30 for 10 mM AMUPol in d$_8$-glycerol/D$_2$O/H$_2$O 60/30/10 ($V/V/V$),[11, 24] and from 205[12] to about 13 (this work, table S3) for 16 mM TEKPol in 1,1,2,2-tetrachloroethane (TCE). Note that, as recently reported, after correction of these values by depolarization and quenching effects,

less drastic decrease in overall enhancement factors have been observed, more in line with the $1/B_0$ dependence.[26] Second, the overall sensitivity gain provided by dinitroxides decreases significantly with increasing spinning frequencies.[21-27] As detailed by Thurber and Tycko and by Mentink-Vigier *et al.*, the MAS-induced modulation of the two electron frequencies leads to a sizeable probability of non-adiabatic electron-electron crossings, which attenuate the spin polarization differences among electrons, subsequently reducing the nuclear spin polarization via CE mechanisms. In the absence of microwaves (μw), this can lead to a depolarization of the nuclei.[26-27] We have recently reported that in solutions of 10 mM AMUPol, while the enhancement factor remains constant from 5 to 40 kHz MAS, the overall NMR sensitivity gain decreases by almost a factor of two.[24]

Enhancements over 100 at 18.8 T (800 MHz ^{1}H resonance frequency) and 40 kHz MAS have been recently obtained using BDPA (*a,γ*-bisdiphenylene-*β*-phenylallyl) in *ortho*-terphenyl as glassy matrix by making use of the Overhauser Effect (OE).[28-29] However, the OE currently requires build-up times on the order of 40 s that mitigate to some extent the gain in overall sensitivity. An important step forward with regard to the field and MAS spinning frequency limitations has been achieved by Mathies *et al.* in 2015. Capitalizing on the pioneering work by Hu *et al.*,[30] who investigated mixtures of TEMPO and trityl radicals to improve the efficiency of the DNP polarization process, Mathies and co-workers introduced a new class of biradicals, TEMTriPols, that link together a nitroxide and a narrow-line trityl radical.[31] The authors highlighted the influence of the electron-electron exchange interaction on the field dependence of the DNP enhancement factor and showed that this enhancement does not decrease with the magnetic field in the same way as observed for dinitroxides. For the best radical in this series, an enhancement of 65 was reported at 18.8 T with a build-up time of 3.7 s. In contrast to nitroxide biradicals, these TEMTriPols do not induce significant depolarization.[31-32] TEMTriPols are soluble in aqueous media and tailored for biological applications. Radicals with similar structures but soluble in organic solvents, have been proposed, yielding enhancements of up to 50 at 9.4 T.[33] In parallel, chiral trityl-nitroxide polarizing agents tethered by a proline linker have been investigated, illustrating again the importance of the magnitude of the exchange interaction in the DNP process.[34]

BDPA-nitroxide radicals are another family of hybrid biradicals that could be suitable candidates for efficient CE DNP at high magnetic field. Using a BDPA moiety as the EPR narrow-line component in place of a trityl radical offers several advantages. First, the electron longitudinal spin relaxation time of BDPA is much longer than that of trityl (around 20 ms for BDPA[35] vs. 1.4 ms for trityl-type radicals[36]) which leads to a more efficient saturation of the EPR line. The *g*-anisotropy of BDPA is also smaller than for trityl-type radicals,[37] leading to a more homogeneous line and a limited broadening at high magnetic field. In 2009, Swager and Griffin described the synthesis of a BDPA-TEMPO biradical where the TEMPO radical was directly linked through an amide bond to the phenyl ring of the BDPA moiety. This radical exhibited a large magnetic exchange interaction (140 MHz), but no DNP measurements were reported.[38] More recently a BDPA and TEMPO biradical covalently bound by a carboxymethylidene has been prepared and evaluated as a polarizing agent for dissolution DNP.[39]

Here we introduce a new family of CE hybrid biradicals in which a BDPA moiety and a nitroxide are chemically tethered. We show that by rationally fine tuning the chemical structures of these

BDPA-nitroxide biradicals, their electronic properties can be significantly modulated, and correlations are established with their DNP performance. In particular, we demonstrate that higher enhancements are obtained by decreasing the length of the linker and by increasing the bulkiness of the substituents at the nitroxide moiety. The best radical in this series, referred to as HyTEK2, combines the advantages of strong magnetic interactions and long nitroxide electron spin relaxation times. With HyTEK2 we observe a proton enhancement $ε_H$ of 185 at 18.8 T for a frozen solution of TCE in a 1.3 mm rotor at 40 kHz MAS, which is the highest DNP enhancement ever obtained at this magnetic field. In 3.2 mm sapphire rotors, this radical gives enhancement factors of over 60 at 18.8 T. The effects of the microwave field inside the MAS rotor and of the probe design are discussed. We then demonstrate that the high DNP efficiency of HyTEK2 is preserved at 21.1 T, the highest field available for MAS DNP today. Finally, we illustrate the performance of these hybrid biradicals in DNP Surface Enhanced NMR Spectroscopy (DNP SENS) at high magnetic field.

The radicals are stable for three months as powders and stable in TCE solution for two weeks, when stored at -18 °C in both cases. Electrospray ionization (ESI) high resolution mass spectra show that the radicals are pure within the limits of detection of the method (90-95 %). No additional signals indicating side products were observed.

2. EXPERIMENTAL SECTION

Sample preparation of radical solutions. 1,1,2,2-Tetrachloroethane (TCE, reagent grade, ≥ 98 %) was purchased from Sigma Aldrich and d_4-methanol from Eurisotop (99.8 % deuteration). Potassium bromide was purchased from Alfa Aesar (> 99 %). All chemicals were used as received if not described otherwise. Free radical solutions were prepared by dissolving the powdered compound in TCE. Samples were filled into 3.2 mm sapphire rotors and capped with silicone plugs, or in 1.3 mm zirconia rotors without plugs. Samples in 3.2 mm rotors were degassed at least 3 times to reduce the concentration of paramagnetic oxygen in the sample.[20] In 1.3 mm rotors, freeze-thaw cycles did not yield any increase in the enhancement, indicating that the rotors are too tight to allow for efficient degassing (data not shown). For measuring enhancements, the polarization build up times without microwave irradiation ($T_{B,OFF}$) and with microwave irradiation ($T_{B,ON}$), a small layer of finely ground KBr was added to the bottom of the rotor in order to monitor the sample temperature via the ^{79}Br nuclear relaxation time.[40] By comparison with enhancements in rotors without any KBr, we could verify that this small amount does not lead to an increase of enhancements by the effect of dielectric particles in the rotor[20] (data not shown). For measurements of absolute signal intensities in the absence of microwaves, rotors were completely filled with KBr crystals and impregnated with a weighed amount of radical solution. This procedure avoids the formation of air bubbles that appear when 1.3 mm rotors are filled with a liquid. The presence of air bubbles in the rotor would indeed falsify the measurement of the absolute signal intensity. The mass of biradical solution in the rotors filled with KBr was around 1-2 mg. The mass of solution was weighed each time and the signal intensity was normalized to the mass of the solution in the rotor.

MAS DNP NMR experiments on bulk radical solutions. The MAS DNP NMR experiments were performed on Bruker Avance III 400 and 800 MHz wide bore as well as on a Bruker 900 US²

2

wide bore spectrometers, equipped with triple resonance 3.2 mm or 1.3 mm low-temperature DNP MAS probes. The samples were irradiated with continuous wave high-power microwaves at a frequency of 263 GHz (9.4 T, 400 MHz [1]H Larmor frequency), 527 GHz (18.8 T, 800 MHz [1]H Larmor frequency) or 593 GHz (21.1 T, 900 MHz [1]H Larmor frequency), with a power stability better than ±1%. The external magnetic field was set to the value of maximum DNP enhancement, corresponding to a microwave irradiation close to the EPR resonance of the BDPA moiety. The μw power was optimized to an output of 40 W at 9.4 T, 5-7 W at 18.8 T (Figure S24), and 9 W at 21.1 T, all values were measured at the bottom of the probe. Solvent carbon-13 T_2' of 32 mM HyTEK2 in bulk TCE solution are reported as a function of the MAS rate in Figure S42.

Spectra acquisition. On samples packed into 1.3 mm zirconia rotors, ^{1}H NMR spectra were recorded for all measurements. In order to attenuate the background probe signal, one-dimensional ^{1}H experiments were acquired using a DEPTH pulse sequence, consisting of a $\pi/2$ pulse followed by two π pulses which are phase cycled according to a combined "EXORCYCLE" and "CYCLOPS" scheme.[41-43] $\pi/2$ pulses of 2.5 μs (100 kHz RF field) were used. At 18.8 T, the background signal of the probe could not be fully suppressed using DEPTH experiments and an additional background correction using TopSpin was applied. In 3.2 mm rotors, ^{1}H enhancements were measured indirectly on the ^{13}C CP signal of the solvent, as the signal of the silicon plug overlapped with that of the solvent in ^{1}H spectra. [1]H build up times without microwave irradiation ($T_{B,OFF}$) or with microwave irradiation ($T_{B,ON}$) were measured with a standard saturation recovery sequence followed by an echo period before signal acquisition under "μw off" and "μw on" conditions, respectively.

Sample temperature. The sample temperature was adjusted by measuring the [79]Br longitudinal relaxation time between the "μw on" and "μw off" experiments and over the whole MAS frequency range.[40] Note that due to heating of the sample by gas friction at fast spinning speeds, and additional heating of the solvent due to μw irradiation, most of the experiments were carried out at temperatures at about 140 K at 18.8 T and about 120 K at 9.4 T, respectively. After the installation of an improved cooling unit, lower temperatures of around 110 K could be reached at 18.8 T. Temperatures are indicated in the legend of the figures. The temperature dependence of the enhancement of HyPTEK was assessed at 18.8 T in a range from 140 to 200 K at both 10 and 40 kHz MAS rate (Figure S25). The enhancements of HyTEK and HyTEK2 were measured at both 110 and 140 K in the spinning frequency range 0 to 40 kHz.

DNP SENS experiments. DNP SENS spectra of impregnated γ-alumina and amorphous aluminosilicates (ASAs) were measured at 18.8 T with an optimized μw output power of 6.5 W (measured at the bottom of the probe) at a MAS rate of 40 kHz with a sample temperature of approx. 115 K during μw irradiation. Both samples were impregnated using the incipient wetness impregnation method.[44] The ASA material was impregnated under inert atmosphere with either with 32 mM TEKPol or 32 mM HyTEK2 in degassed and dried TCE, and packed in a 1.3 mm zirconia rotor inside the glove box. For the [27]Al CP experiments, a [27]Al radio-frequency (RF) field of 25 kHz was applied during a contact time of 0.8 ms, while the ^{1}H RF field was ramped from 17.5 to 25 kHz. For the [29]Si CP spectra, the [29]Si RF field was approx. 50 kHz while the ^{1}H RF field was ramped from 65 to 95 kHz during a contact time of 3 ms. In all cases, 100 kHz ^{1}H SPINAL-64 decoupling was applied during

acquisition.[45] [29]Si CPMG acquisition was carried out with [29]Si π pulses of 5.6 μs and an echo time of 1 ms. A total of 60 echoes was recorded. Spinal-64 decoupling at 150 kHz was applied during the whole acquisition period. The silicon-29 T_2' value was measured from a [29]Si CP Hahn-echo experiment. Here, we define $T2'$ as the time constant that can be measured in a spin-echo experiment.[46]

EPR experiments. Low temperature W-band EPR measurements were carried out on a Bruker E680 spectrometer at a μw frequency of 94 GHz (W-band) and a temperature of 105 K, on 0.1 mM frozen solutions of the hybrid biradicals in TCE. $\pi/2$ and π pulses of 52 ns and 104 ns were used, respectively. EPR spectra were recorded using field-dependent echo detection (echo-detected EPR). Longitudinal relaxation times were recorded with the inversion recovery sequence, and transverse relaxation times using a variable delay Hahn echo sequence. The Hahn echo delay time for the inversion recovery detection and the initial echo delay in the transverse relaxation measurements was set to 400 ns. The data were fitted with a stretched exponential to account for a distribution of the values, in some cases a biexponential fit was applied (see section 2 in the SI). The first moment of this distribution is indicated as the mean value (for details see section 2 in the SI). The relaxation curves were recorded at the EPR intensity maxima of the BDPA and nitroxide moieties. Solution-state X-band (9.4 GHz) continuous-wave (CW) EPR measurements were carried out on a Elexsys E600 spectrometer at 295 K with 0.5 mM solutions of the free radicals in TCE, degassed in three freeze-thaw cycles. The simulations were performed using the EasySpin EPR simulation package (MATLAB).[47]

3. RESULTS AND DISCUSSION

Rational design of the investigated biradicals. In the series of hybrid biradicals investigated in this work (Figure 1), first the length of the linker tethering the BDPA and the nitroxide moieties was varied. The distance between the two free electrons has been shown to be an important parameter for CE DNP.[10-12, 17, 31, 48] Notably, reduced distances lead to an increase in the electron-electron magnetic interactions (the dipolar and/or exchange coupling interactions) that play a key role in the overall efficiency of the polarization transfer mechanism under MAS.[21, 25, 48] Biphenyl, phenyl and methylene linkers were considered. They correspond to electron-electron distances of respectively around 21, 17 and 12 Å (table S1). Dipolar and exchange interactions were estimated from point dipole approximations and from solution CW EPR spectra, respectively (see Table S1). The functionalization of the BDPA moiety was performed via a carbonyl group at the phenyl position where nearly no electron spin density is located, to minimally perturb the electron spin properties of the BDPA radical.

Second, different nitroxide moieties were introduced in order to modulate the nitroxide electron relaxation properties. In dinitroxides, we indeed previously observed that longer electron relaxation times result in higher enhancements, likely due to a better saturation of the electronic transitions.[10-12] Here, although the optimal DNP enhancements are obtained upon μw saturation at the resonance frequency of BDPA (see below), the relaxation times of the nitroxide moiety are expected to impact the overall polarization transfer efficiency. Modulating the relaxation times of the non-saturated electron has not been investigated so far for hybrid trityl-nitroxide biradicals. The biradicals in the series differ by the substitution in the α-position to the nitroxide moiety, from simple methyl

3

groups (Figure 1b and 1c, Hy-1 and Hy-2) to bulkier spiro-tetrahydropyranyl (Figure 1d), 4-phenyl spirocyclohexyl (Figure 1e) and 3,5-diphenyl spirocyclohexyl moieties (Figure 1f), reminiscent of AMUPol,[11] TEKPol[12] and TEKPol2.[13] We have dubbed the latter radicals HyPTEK (Hybridized Phenyl-linked TEKPol-like), HyTEK (Hybridized TEKPol-like) and HyTEK2 (Hybridized TEKPol2-like).
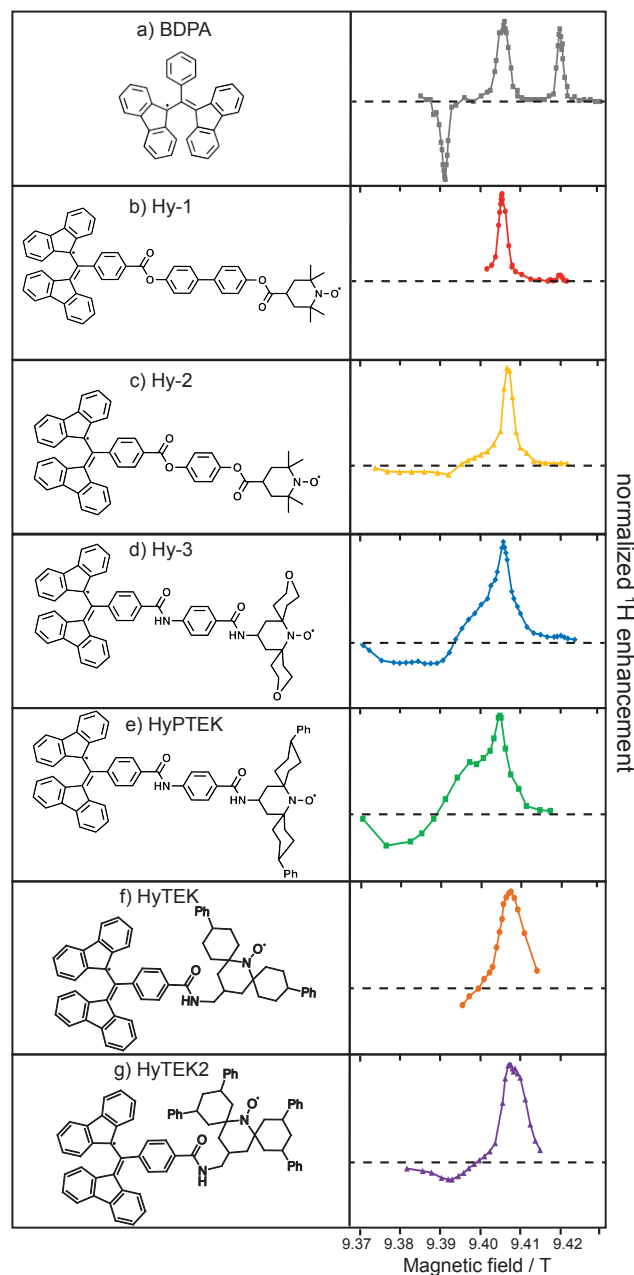

Figure 1. Molecular structures of BDPA and hybrid BDPA-nitroxide biradicals together with their DNP enhancement field profiles for 32 mM (a, c-g) or 16 mM (b) in TCE. The data were recorded at 9.4 T, 8.0 kHz MAS frequency and ~115 K sample temperature. The DNP enhancement profiles are normalized. Dashed lines on the right indicate the x axis at $\varepsilon = 0$.

Electronic relaxation properties of the hybrid biradicals.

Figure 2 shows the W-band (95 GHz) echo-detected EPR spectra of all radicals in TCE at 105 K. For all these radicals, except for HyTEK and HyTEK2, we can clearly recognize the narrow peak of BDPA at about 3.35 T, as well as the broad, asymmetric feature ranging from 3.345 to 3.365 T corresponding to the nitroxide moiety. For the radicals Hy-1 and Hy-2, the nitroxide feature is extremely weak due to the rapid relaxation of the TEMPO units (for better visibility of this feature, see Figure S26). The low temperature spectra of Hy-1, Hy-2, Hy-3 and HyPTEK do not show any indication of a broadening of the BDPA line due to the spin-spin interactions between the two radical moieties. In contrast, in HyTEK and HyTEK2, the BDPA line appears significantly broadened, which possibly originates from both a stronger spin-spin coupling due to the shorter distance between the two electrons and possibly a larger g-anisotropy than in the other radicals.
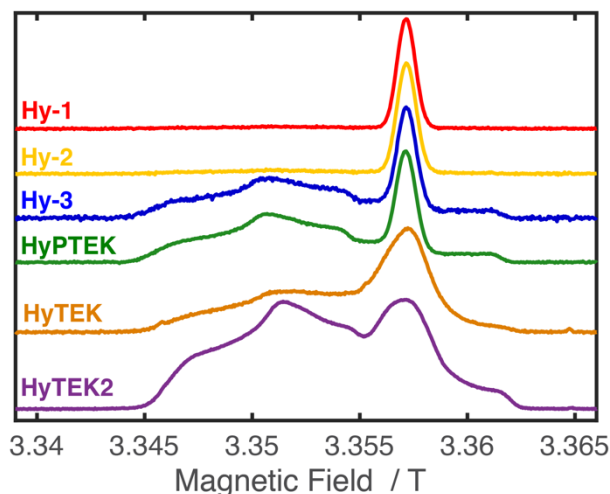
Figure 2: W-band (~94 GHz) echo-detected EPR spectra of 100 μM solutions of all hybrid biradicals in TCE at 105 K. The magnetic field values for the EPR spectra were subjected to constant shifts to compensate for the variations in the resonator frequency for different samples.

Figure S27a shows the EPR spectra (X-band, 9 GHz) of these radicals in solution, where the isotropic molecular tumbling averages out most of the anisotropic interactions. Biradicals Hy-1 to HyPTEK do not show any evidence of the presence of a strong isotropic exchange interaction, as the three EPR lines of the nitroxide and the hyperfine structure of the BDPA resonance are clearly observed. The solution EPR spectra of HyTEK and HyTEK2 are very different suggesting the presence of a significant isotropic exchange coupling J, of the order of the nitroxide ^{14}N hyperfine interaction (around 40 MHz).[49] These spectra were tentatively fitted as shown in Figure S27 (b) and (c). Reasonable fits were obtained using two components with two different J values, the largest component having a J value of the order of 50 MHz, which is in agreement with the estimated values in table S1. However, as the methylene group between the two radical moieties has some conformational flexibility that will lead to a distribution of magnetic interactions, the fitted values of the J-coupling should be regarded as a rough estimation.

The electronic inversion recovery (T_{ir}) and phase memory times (T_m) were determined separately at the frequencies of the two radical moieties (Table 1). For the biradicals Hy-1 and Hy-2, the T_{ir} were too short to be determined in a spin echo experiment. In the nitroxides with bulkier and rigid substituents, the T_{ir} are still at

least an order of magnitude smaller than those of the BDPA moiety. The T_{ir} of the BDPA moiety range from 3.7 to 5.1 ms for hybrid radicals with biphenyl or phenyl linkers (Hy-1, Hy-2, Hy-3 and HyPTEK) and are considerably shorter than the T_{ir} measured for a pure BDPA solution (approx. 20 ms for 15 mM BDPA in sulfolane:DMSO, 1:1, V:V),[35] in accordance with the presence of a dipolar coupling between the two unpaired electrons. A similar effect was observed by Michaelis *et al.* in a mixture of BDPA and faster relaxing trityl radicals.[36] For HyTEK and HyTEK2, the T_{ir} of the BDPA moiety are similar and both strongly reduced (1.9 and 1.5 ms, respectively), further supporting the presence of stronger spin-spin interactions in these biradicals. At the nitroxide moiety, both the inversion recovery times and the phase memory times increase with the bulkiness of the nitroxide substituents, as already observed for dinitroxides biradicals,[10, 12-13] with an exception for the relative T_{ir} values of Hy-3 and HyPTEK, where this trend is not seen. Importantly, the relaxation times of the nitroxide moiety of HyPTEK and HyTEK, which corresponds in both cases to a TEK-Pol moiety, are similar, while being significantly shorter than those of HyTEK2, which bears the bulkier TEKPol2-like substituents.

Table 1: Electronic inversion recovery T_{ir} and phase memory times T_m of 0.1 mM hybrid biradicals in TCE solutions. The relaxation parameters of the TEMPO moieties of Hy-1 and Hy-2 were too short to be determined with an echo experiment.

radical	T_{ir} / ms BDPA	T_{ir} / ms nitroxide	T_m / µs BDPA	T_m / µs nitroxide
Hy-1	4.1 ± 0.1	n.d.	5.1 ± 0.1	n.d.
Hy-2	3.7 ± 0.1	n.d.	5.1 ± 0.1	n.d.
Hy-3	5.1 ± 0.1	0.27 ± 0.01	4.7 ± 0.1	3.0 ± 0.1
HyPTEK	4.5 ± 0.1	0.26 ± 0.01	4.6 ± 0.1	3.3 ± 0.1
HyTEK	1.9 ± 0.1	0.25 ± 0.01	3.2 ± 0.1	3.4 ± 0.1
HyTEK2	1.5 ± 0.1	0.35 ± 0.01	3.3 ± 0.1	4.4 ± 0.1

DNP field profiles.

As in the low temperature W-band EPR spectra, the field profiles of the hybrid radicals at 9.4 T reported in Figure 1 show two distinct features. In analogy to TEMTripol,[31] we attribute the sharp, symmetric positive enhancement between 9.40 and 9.41 T to intramolecular BDPA-nitroxide CE. The position of this maximum enhancement corresponds to that of the BDPA OE enhancement (Figure 1a) and thus to the irradiation at the BDPA EPR frequency. Broad asymmetric, positive and negative enhancement lobes are observed (Figure 1c-f) between 9.37 T and 9.41 T that arise essentially from two contributions: intramolecular nitroxide-BDPA CE due to irradiation at the nitroxide resonance and intermolecular CE between two nitroxide moieties. The relative intensity of the intermolecular nitroxide-nitroxide CE is weak for Hy-2 with respect to the bulkier radicals Hy-3 and HyPTEK, in line with analogous observations of a more efficient CE in long relaxing dinitroxides.[12-13] The intramolecular nitroxide-BDPA CE which occurs upon saturation of the nitroxide resonance shows a negative minimum at about 9.392 T corresponding to the simplified matching condition $\omega_n \cong \omega_{e1} - \omega_{e2}$, and is clearly visible for radicals Hy-2, Hy-3 and

HyTEK2. The irradiation of the nitroxide radical yields however much lower CE DNP enhancements. This asymmetry in the field profile has already been observed in TEMTriPol.[31] Note that µw irradiation at the BDPA EPR frequency could also generate an additional contribution due to OE DNP of the BDPA moiety alone. In our experimental conditions however, an OE enhancement of 5 was measured for a solution of 32 mM BDPA in TCE at 9.4 T (Figure 3), suggesting that the OE contribution from BDPA is very small and will not have a substantial impact on the performance of the hybrid radicals. We finally observe that the enhancement profiles at the BDPA EPR resonance of HyTEK and HyTEK2 are significantly broadened (Figure 2, bottom traces). This broadening originates from a larger g-anisotropy than in the other radicals and possibly from stronger spin-spin interactions. Such a broadening has been observed previously by Dane *et al.*[38] and by Mathies *et al.*[31]

DNP enhancements at 9.4 and 18.8 T and correlations with the structures.

The biradical concentration was varied for two polarizing agents in the series, namely for Hy-3 between 16 and 64 mM and for HyTEK2 between 5 and 48 mM (Figure S28), and the corresponding DNP enhancements were measured at 18.8 T in bulk solutions of TCE. Molecular concentrations of 32 mM appear to be optimal; higher concentrations did not improve the enhancements or led to a drop. Here we note that the 32 mM concentration was optimized for a homogenous solution and that the optimal radical concentration will likely be different for practical applications. For DNP Surface Enhanced NMR Spectroscopy (DNP SENS),[2, 44] it has recently been shown that the optimum radical concentration will depend on many parameters, like the specific surface area of the material, the affinity of the radical for the surface or the proton content at the surface.[50-52] In particular, a high concentration may have a detrimental impact on transverse coherence lifetimes of heteronuclei or may increase the quenching effect in some applications, notably in cases where the radicals are in close contact with the investigated surface. On the contrary, for remote polarization of microcrystalline organic solids by DNP, high radical concentrations may be preferred because they can minimize the surface build-up time, which helps to maintain a high level of polarization at the surface of microcrystalline particles. It is therefore difficult to determine a priori the most suitable radical concentration in real applications. All the following measurements were done in bulk solutions of TCE at a radical concentration of 32 mM.

Proton enhancements in bulk frozen solutions of TCE were measured as a function of field and MAS frequency in prototype 1.3 mm probes. At 9.4 T (Figure 3) the enhancements rapidly increase up to 10 kHz MAS frequency for all biradicals in the series, and continue to increase for Hy-3, HyPTEK and HyTEK2. The lowest enhancements are obtained for Hy-1, with a maximum of $\varepsilon_H = 24$ at 5 kHz. We attribute this poor efficiency to the long linker which results in an average distance of ca. 21 Å between the carbon atom at the edge of the allyl radical and the nitrogen atom of the nitroxide. The long distance reduces the magnetic interactions which play a crucial role in the efficiency of the MAS CE.[21, 27] For radicals Hy-2, Hy-3 and HyPTEK, which have a shorter tether (17 Å), the enhancements are significantly higher and additionally improve with the bulkiness of the nitroxide moiety, in line with observations for dinitroxides.[10, 12-13] Although HyTEK2 was measured at a slightly lower temperature, data in Figure 3 show that it clearly performs better than the other radicals investigated at 9.4 T. This radical

5

exhibits the shortest linker, together with HyTEK, with an average electron-electron distance of 13 Å, as well as the bulkiest ligands. As discussed previously, the short distance between the two electrons introduces strong dipolar and exchange interactions, while the bulky and rigid functional groups lead to long electronic relaxation times at the nitroxide moiety as evidenced by the EPR data. The MAS dependence of the enhancements of HyTEK was not investigated at this field. For all radicals, we observe that the nuclear polarization build-up times in absence and presence of μw ($T_{B,OFF}$ and $T_{B,ON}$, respectively) increase linearly with spinning frequency (Figures S29-S33).
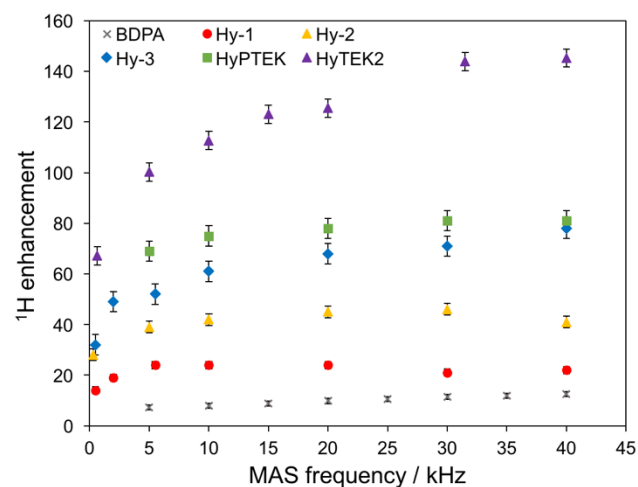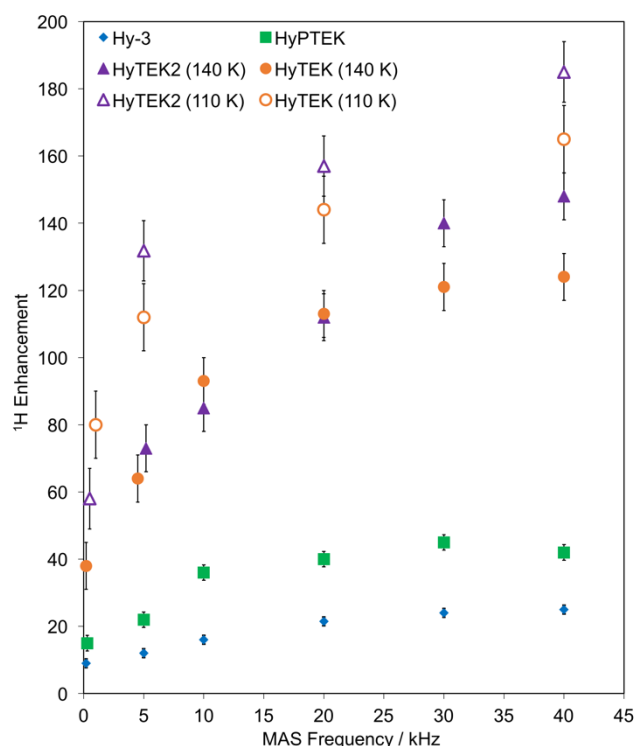

Figure 3. MAS dependence of proton enhancement ε_H of hybrid biradicals (32 mM in TCE) at 9.4 T in a 1.3 mm rotor. Sample temperatures: 122 ± 5 K for Hy-1, Hy-2, Hy-3 and HyPTEK solutions, 113 ± 3 K for HyTEK2 solution.

The performances of the three most efficient radicals at 9.4 T and of HyTEK were investigated at 18.8 T (Figure 4, filled symbols). As at lower magnetic field, the enhancements, $T_{B,OFF}$ and $T_{B,ON}$ increase with faster spinning (Figure 4 and Figures S34-S38). More importantly, we observe again that the highest enhancements are obtained for the biradicals having the shortest linker: HyTEK and HyTEK2 indeed yield enhancement factors more than 3 times higher than HyPTEK and Hy-3, with maximum values of respectively 124 and 142 at 40 kHz MAS and 140 K. In addition, HyTEK2 outperforms HyTEK, which differs from HyTEK2 only by the less bulky ligands. We note that these enhancements are much higher than what has been measured before for BDPA in TCE (23 at 40 kHz MAS), confirming that the OE is not the main DNP mechanism here (Figure S39, data from Chaudhari et al.).[29] Also, these enhancements largely outperform those obtained with TEKPol under similar experimental conditions (less that 10 at 40 kHz MAS, Figure S39).

The rather elevated temperatures in these series of experiments were due to hardware limitations. After the installation of an improved cooling unit, we were able to measure the enhancements for the two best performing biradicals at a much lower temperature of around 110 K (open symbols), which corresponds to the standard temperature usually employed for biradical testing. Again, HyTEK2 gives higher enhancements than HyTEK (185 versus 166), further confirming the importance of long electronic relaxation times at the nitroxide moiety in these hybrid biradicals. In conclusion, the systematic investigations that we performed at 9.4

and 18.8 T reveal clear correlations between the chemical structure of the hybrid BDPA-TEMPO biradicals and their DNP performance. They notably highlight the fact that to achieve sizeable enhancements at 18.8 T, both long nitroxide electronic relaxation times (comparable or longer to those measured for TEKPol[12]) and strong dipolar and exchange interactions are necessary. Note that a hybrid biradical with an even shorter linker (one CH2 group less, Figure S40) yielded a lower enhancement factor than HyTEK and HyTEK2 (Figure S41), suggesting that there is an optimal value for the electron-electron couplings in this series of biradicals. At 110 K, enhancements of up to 185 were reached with HyTEK2, which is by far the best enhancement ever measured at a magnetic field of 18.8 T. Notably, the DNP performance of HyTEK2 is significantly better than that recently observed for the OE DNP with BDPA in OTP, for which an enhancement of 105 was reported at 18.8 T and 40 kHz MAS frequency.[29] Additionally, the build-up times are much shorter in this system: 3.3 s for HyTEK2 vs. 43.5 s for BDPA in OTP at 40 kHz MAS and 18.8 T in a 1.3 mm rotor.

Figure 4. MAS dependence of proton enhancement ε_H of Hy-3, HyPTEK, HyTEK and HyTEK2 (32 mM in TCE) at 18.8 T in a 1.3 mm rotor. Sample temperatures: 140 ± 3 K for Hy-3, 147 ± 3 K for HyPTEK, 140 ± 2 K or 110 ± 3 for HyTEK, 140 ± 2 K or 110 ± 3 K for HyTEK2.

Influence of the rotor size on the enhancements.

The enhancements of HyTEK2 were studied in both 3.2 and 1.3 mm rotors and at 9.4 and 18.8 T (Table S2). At 9.4 T the enhancements do not differ between the two rotor sizes. Interestingly, at 18.8 T, ε_H increases from 65 in a 3.2 mm rotor to 138 in a 1.3 mm rotor at 10 kHz MAS frequency. We hypothesize that the microwave field in the sample is on average higher in amplitude in the small rotor at the higher magnetic field. It has already been shown that the microwave distribution is inhomogeneous in 2.5, 3.2 and 4 mm rotors[20, 53-54] and that the addition of dielectric particles improves enhancements in 3.2 mm rotors at 9.4 T by a factor of two,

6

due to scattering, diffraction, and amplification of the microwave field in the sample.[20] As shown in the SI, we estimated the microwave field distribution at 9.4 T and 18.8 T in the specific probe design we have, by using finite element simulations.[20, 53] The simulation show that at 9.4 T the average microwave magnetic field is essentially the same in the active volume of both rotor sizes. At 18.8 T in the 1.3 mm rotor the average field is increased by a factor of 48 % with respect to a 3.2 mm rotor, due to different probe geometry, which is in excellent agreement with the enhancement measurements (Table S2 and Figure S43). The increased average field in the 1.3 mm probe is partly due to the presence of a PTFE lens, which focusses the microwave beam on the rotor. Additionally, we predict that the change at 9.4 T should be negligible, as we also observed. These results show that the absolute value of the enhancement is strongly dependent on the microwave field inside the rotor, and may vary from one probe design to another. We note here that at 18.8 T, HyTEK2 in TCE gives an enhancement that is comparable to that of TEMTripol in a glycerol/water mixture.[31]

DNP enhancements at 21.1 T.

The performance of HyTEK2 was evaluated at 21.1 T. At this high magnetic field, an OE enhancement of 73 has recently been published on a solution of BDPA in OTP in a 3.2 mm rotor at 10 kHz MAS.[55] For HyTEK2 at this field we obtained an enhancement of 64 under similar experimental conditions (Figure S44). This value is comparable to the one obtained at 18.8 T in the same rotor size (65 at 10 kHz MAS), but lower than values obtained in smaller diameter rotors. This result shows that the good performance of HyTEK2 is preserved at the highest magnetic field available today for DNP MAS NMR experiments.

Increased DNP efficiency with fast MAS.

The trend of increasing ε_H as a function of MAS has been observed before in OE DNP with BDPA in OTP.[29] In that study, it was attributed to the presence of a low concentration of relaxation sinks, that compete with the polarization sources. With increasing MAS rates, the ^{1}H-^{1}H spin diffusion rate is progressively reduced, thus isolating the sinks from the bulk and leading to an overall increase in both nuclear polarization and build-up times.[29] A weak dependence of the DNP build-up as a function of MAS was also observed using AMUPol in d_8-glycerol/D_2O/H_2O 60/30/10 ($V/V/V$).[24] In general in dinitroxides, constant or decreasing enhancements have so far been reported as a function of the MAS frequency at frequencies larger than 2-3 kHz.[12, 24, 26, 32] This is thus the first time that a sizeable increase with MAS of both enhancement and build-up time is observed for a CE biradical.

Thurber and Tycko, as well as Vega and coworkers, developed a theoretical model to explain how the DNP CE mechanism intrinsically depends on the MAS frequency.[21, 25] In this model, the spinning frequency regulates the degree of adiabaticity of the energy level crossings that occur when the resonance of one of the two electrons periodically matches the microwave frequency, when the two electron frequencies match, or when the three-spin CE condition is fulfilled. As a consequence, the simulations predict that for dinitroxides, the overall efficiency of polarization transfer to nuclei will decrease for high MAS frequencies.

For hybrid biradicals having one narrow EPR line component, like TEMTriPols, the degree of adiabaticity at the three energy level crossings will be less affected by increasing MAS frequencies with respect to dinitroxides. TEMTriPol-1 shows indeed a DNP enhancement that is almost stable above 5 kHz of MAS, and a complete absence of depolarization (see below).[32] Similarly, for the BDPA-nitroxide series introduced here, we expect CE enhancements that decrease little or not with the MAS frequency, as these biradicals contain one narrow EPR line component. What is more, we actually observe that they increase with the spinning frequency. We suggest that this trend is governed by spin-diffusion processes similar to those proposed for OE DNP described above. This hypothesis is supported by the lengthening of the DNP build-up times with increasing MAS frequency (Figures S29-S38). We therefore applied the same source-sink model as for OE in BDPA to simultaneously fit the experimental MAS dependence of ε_H and $T_{B,ON}$ observed at 18.8 T (details in the SI, section 5). Figure S45 reports the fit of the enhancement versus MAS for Hy-3, HyPTEK and HyTEK2. The good agreement we observed in these fits indicates that the source-sink model can explain the experimental trends, especially at fast MAS. The fits reported here were obtained with a concentration of sinks of 49 μM in TCE for the curves of all examined polarizing agents. The same sink concentration was found for the three best biradicals which supports the hypothesis that the polarization sinks could be a solvent paramagnetic impurity, such has dissolved oxygen. For comparison, a sink concentration of 14 μM was obtained for BDPA in the OTP matrix.[29] The higher concentration of the relaxation sinks estimated for hybrid biradicals in TCE with respect to BDPA in OTP, which could be rationalized for example by the higher solubility of oxygen in TCE, makes it possible to observe a sizeable MAS dependence of the enhancements and of the build-up times even if the $T_{B,ON}$ are relatively short.

A further refinement of the model will include the simulation of the intrinsic CE MAS dependence, using detailed information on the electronic properties of these hybrid biradicals coming from a deeper and detailed EPR characterization, and will be a subject of future work.

Contribution factor and overall sensitivity gain.

The contribution factor takes into account both paramagnetic quenching and depolarization effects and can be regarded as the apparent fraction of the nuclei in the sample that contributes to the signal in the presence of the biradical and in the absence of microwaves.[21, 26, 56-57] Contribution factors θ of 67 % for Hy-3, 64 % for HyPTEK and 71 % for HyTEK2 were measured at 18.8 T and were constant over a MAS frequency range from 5 to 40 kHz (Figure S46). In the static case, a reliable measurement of this contribution factor could not be done at 18.8 T due to the large probe background. It is therefore difficult to disentangle the effect of depolarization and of paramagnetic quenching. However, our data clearly indicate that increasing the MAS rate does not lead to more pronounced depolarization effects over a frequency range of 5-40 kHz, in contrast to what has been observed with AMUPol.[24] At 9.4 T, a contribution factor of about 50 % is observed for HyTEK2, which additionally shows a small decrease with the MAS rate (Figure S47). At 9.4 T, the intermolecular nitroxide-nitroxide CE contributes to the overall enhancement, as can be seen from the field profiles (Figure 1). This nitroxide-nitroxide CE mechanism is also expected to lead to some depolarization and lower contribution

factor with increasing MAS frequencies. This may explain the trend observed at this field in Figure S47.

The overall sensitivity gain is proportional to the enhancement factor, to the contribution factor and to the inverse of the square root of the polarization build-up time (as detailed in the SI, section 4).[2, 56-57] For the BDPA-nitroxide biradicals, the enhancements significantly increase with the MAS frequency, while on one hand the DNP build up times become only moderately longer and on the other hand the contribution factors remain roughly constant over the 5 to 40 kHz spinning regime. In Figure S48, we show that for HyTEK2, this translates in an overall sensitivity gain that increases with the MAS rate at 18.8 T. At 18.8 T and 40 kHz MAS, HyTEK2 yields an overall sensitivity gain of 676 compared to a room temperature NMR experiment done without polarizing agent and μw irradiation (Table S3). For comparison, AMUPol and TEKPol yield overall sensitivity gains of 153 and 43. Alternatively, the effective enhancement per square root of time (see section 4 in SI)[32] can be calculated, which gives a value of 72 for HyTEK2 (Table S3), compared to 10 for AMUPol and 4 for TEKPol under comparable conditions.

DNP SENS on alumina and silica-alumina surfaces.

The potential of this new series of biradicals for DNP at high magnetic field is illustrated with the acquisition of DNP SENS spectra of various materials containing quadrupolar nuclei. Both γ-alumina (surface area of 180 m^2/g) and amorphous aluminosilicates (surface area of 140 m^2/g) were investigated. Both materials have already been studied using DNP SENS at 18.8 T with TEKPol as polarizing agent.[58-60] Perras *et al.* have recently investigated the optimum radical concentration for DNP SENS as a function of the surface area of a given material. They demonstrated that for alumina materials containing 5 % silica (Siral-5) and a surface area of about 150 m^2, a TEKPol concentration of around 25 mM was optimal for the absolute signal gain per unit of time.[51] As the materials used in this study show similar surface areas, we chose a HyTEK2 concentration of 32 mM for the impregnation.

For γ-alumina, a solvent enhancement of 50 was obtained at 18.8 T and 40 kHz MAS rate, by comparing the ^1H signal intensity with and without microwave irradiation. A surface enhancement of 46 was measured from the ^{27}Al CP spectra. In this spectrum highlighting the surface species, Al(IV) with a maximum at 67 ppm, Al(VI) at 9 ppm and a smaller amount of Al(V) sites at 35 ppm are clearly visible (Figure S49).[61-63] By impregnation with a 32 mM solution of TEKPol in TCE, much lower enhancements of 12 for the solvent and of 15 for the alumina surface were obtained (Figure S49), further illustrating the advantage of using HyTEK2 at high field.

Amorphous aluminosilicates (ASA-1 and ASA-2)[59] were also investigated. These materials are ubiquitous as catalyst supports and as catalysts themselves due to their high acid and base activity.[64-66] The materials used in this study were produced by grafting of a silicon precursor on an amorphous alumina surface with subsequent thermal treatment forming a submonolayer of silica-alumina for ASA-1 and a layer for ASA-2 on an alumina surface (details of the synthesis see in the SI, section 1). Here we note that these are water-sensitive materials that could not be impregnated with an aqueous solution of water-soluble radicals such as AMUPol or TEMTriPol. By impregnation of ASA-1 with HyTEK2 in TCE, a solvent enhancement of 86 was achieved, which again outperforms the impregnation with TEKPol in TCE by a factor of four (Figure 5). In parallel, the signal

to noise ratio after 1024 scans, normalized to the mass of ASA-1 in the rotor, is three times higher for HyTEK2 than for TEKPol, confirming the superior performance of this hybrid biradical at this high magnetic field. Due to the low signal intensity, ^{27}Al CP spectra without microwave could not be recorded. Again, the three surface sites of alumina are visible. We extracted the quadrupolar constants C_Q, the width of chemical distribution and the isotropic shifts from this spectrum (Table S4 and Figure S50). Al(IV) at 64.8 ppm (isotropic shift) exhibits the largest C_Q of 6.5 MHz as well as the largest width of chemical distribution $\Delta\delta$ of 6.5 ppm, Al(V) at 29.0 ppm and Al(VI) at 4.5 ppm show considerably narrower signals, in line with smaller C_Q and smaller linewidths. We note that the Al(V) signals are present in the spectrum with a high resolution and in high intensity, compared to previous studies at 600 MHz.[59]

Despite the low content of silicon on the surface (1 to 2 %), the high enhancement also allowed us to record a ^{29}Si CPMG spectrum on ASA-2 with a good signal-to-noise ratio (Figure S51). The combination of fast MAS (40 kHz) with high-power heteronuclear decoupling (150 kHz) leads to long transverse coherence lifetimes (^{29}Si T_2' of 27 ms) so that an additional substantial sensitivity gain is obtained with CPMG acquisition.

Finally, we also performed ^{29}Si and ^{17}O DNP-SENS experiments on partially ^{17}O-enriched silica, impregnated with a 16 mM solution of HyPTEK in TCE in a 3.2 mm rotor at 18.8 T (Figure S52). All these application studies demonstrate the potential of this new family of polarizing agents for DNP SENS of challenging materials at high magnetic field.
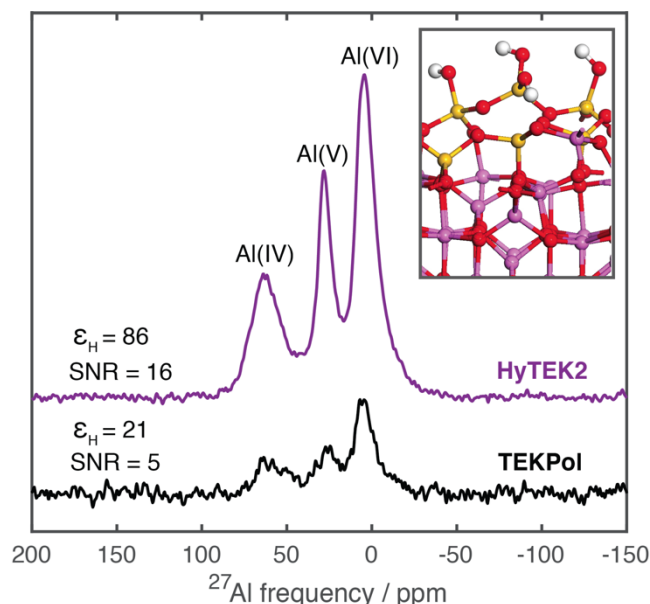
Figure 5: ^{27}Al CP spectrum of the aluminosilicate ASA-1 impregnated with solutions of 32 mM of HyTEK2 (a) and 32 mM of TEKPol (b) in TCE at 18.8 T (527 GHz electron Larmor frequency) at 40 kHz MAS frequency in 1.3 mm zirconia rotors. Both spectra are recorded under μw irradiation. The signal to noise ratios are indicated for 1024 scans and for a same experimental time (1.4 h with a recycle delay of 5 s) and normalized to the mass of the aluminosilicate in the rotor. Inset: Schematic representation of the alumina-silica interface, reproduced from Chizallet *et al.*[67] White: hydrogen, yellow: silicon, red: oxygen, purple: aluminium. A higher silicon content is represented here for better visibility.

Conclusion.

We have introduced a new series of CE hybrid BDPA-nitroxide biradicals suitable for DNP enhanced solid-state NMR at high magnetic field. In this series, we varied the linker length between the two moieties as well as the functionalization of the nitroxide unit. First, by varying the linker length, the electron-electron interactions have been modulated. We observed that the CE efficiency increases with larger exchange and dipolar interactions. In line with prior work, we show that by increasing the bulkiness of the nitroxide ligands, nitroxide electronic relaxation times are increased, which further improves the CE efficiency. The best biradical in this series, HyTEK2, shows sizable exchange interactions and exhibits the longest electronic relaxation times at the nitroxide moiety in the series. This biradical performs extremely well at very high magnetic fields, with signal enhancements of up to 185 at 18.8 T in 1.3 mm rotors where the microwave field distribution is more favorable than in 3.2 mm rotors. Enhancements of up to 65 were measured at 21.1 T in a 3.2 mm rotor, that are significantly higher than those reported for AMUPol (typically around 20 at this field).

Additionally, depolarization effects are reduced in these hybrid biradicals and the absolute sensitivity gains increase with MAS frequency. The peculiar combination of small g-anisotropy for one of the two unpaired electrons, the sizeable electron-electron couplings and the long electron relaxation times at the nitroxide moiety are key features that explain the outstanding performance of HyTEK2 with respect to dinitroxide polarizing agents at high magnetic fields. Nevertheless, we also observe that the performance of the HyTEK2 biradical is also dependent on the probe design, and in particular on the microwave power in the sample. A tailored instrument design could help to further increase the DNP efficiency at high field.

ASSOCIATED CONTENT

Supporting Information. Additional tables and figures as well as synthetic details are available free of charge via the Internet at http://pubs.acs.org."

AUTHOR INFORMATION

Corresponding Author

* moreno.lelli@unifi.it, anne.lesage@ens-lyon.fr, lyndon.emsley@epfl.ch, olivier.ouari@univ-amu.fr

Present Addresses

†CSIR-Central Food Technological Research Institute, Mysore, India
$ Department of Chemistry, 1605 Gilman Hall, Ames, Iowa 50011-1021

Author Contributions

The manuscript was written through contributions of all authors. / All authors have given approval to the final version of the manuscript.

Notes

The authors declare no competing financial interest.

REFERENCES

1.   Ni, Q. Z.; Daviso, E.; Can, T. C.; Markhasin, E.; Jawla, S.; Swager, T. M.; Temkin, R. J.; Herzfeld, J.; Griffin, R. G., *Acc. Chem. Res.* **2013,** *46* (9), 1933-41.

2.   Rossini, A. J.; Alexandre, Z.; Lelli, M.; Lesage, A.; Copéret, C.; Emsley, L., *Acc. Chem. Res.* **2013,** *46* (9), 1942-51.

3.   Becker-Baldus, J.; Bamann, C.; Saxena, K.; Gustmann, H.; Brown, L. J.; Brown, R. C. D.; Reiter, C.; Bamberg, E.; Wachtveitl, J.; Schwalbe, H.; Glaubitz, C., *Proc. Natl. Acad. Sci. USA* **2015,** *112* (32), 9896-901.

4.   Berruyer, P.; Lelli, M.; Conley, M. P.; Silverio, D. L.; Widdifield, C. M.; Siddiqi, G.; Gajan, D.; Lesage, A.; Copéret, C.; Emsley, L., *J. Am. Chem. Soc.* **2017,** *139*, 849-55.

5.   Märker, K.; Pingret, M.; Mouesca, J.-M.; Gasparutto, D.; Hediger, S.; De Paëpe, G., *J. Am. Chem. Soc.* **2015,** *137* (43), 13796-99.

6.   Pump, E.; Viger-Gravel, J.; Abou-Hamad, E.; Samantaray, M. K.; Hamzaoui, B.; Gurinov, A.; Anjum, D. H.; Gajan, D.; Lesage, A.; Bendjeriou-Sedjerari, A.; Emsley, L.; Basset, J.-M., *Chem. Sci.* **2017,** *8* (1), 284-90.

7.   Rossini, A. J.; Zagdoun, A.; Hegner, F.; Schwarzwälder, M.; Gajan, D.; Copéret, C.; Lesage, A.; Emsley, L., *J. Am. Chem. Soc.* **2012,** *134* (40), 16899-908.

8.   Maly, T.; Debelouchina, G. T.; Bajaj, V. S.; Hu, K. N.; Joo, C. G.; Mak-Jurkauskas, M. L.; Sirigiri, J. R.; van der Wel, P. C.; Herzfeld, J.; Temkin, R. J.; Griffin, R. G., *J. Chem. Phys.* **2008,** *128* (5), 052211.

9.   Matsuki, Y.; Maly, T.; Ouari, O.; Karoui, H.; Le Moigne, F.; Rizzato, E.; Lyubenova, S.; Herzfeld, J.; Prisner, T.; Tordo, P.; Griffin, R. G., *Angew. Chem. Int. Ed.* **2009,** *48* (27), 4996-5000.

10.   Zagdoun, A.; Casano, G.; Ouari, O.; Lapadula, G.; Rossini, A. J.; Lelli, M.; Baffert, M.; Gajan, D.; Veyre, L.; Maas, W. E.; Rosay, M.; Weber, R. T.; Thieuleux, C.; Copéret, C.; Lesage, A.; Tordo, P.; Emsley, L., *J. Am. Chem. Soc.* **2012,** *134* (4), 2284-91.

11.   Sauvée, C.; Rosay, M.; Casano, G.; Aussenac, F.; Weber, R. T.; Ouari, O.; Tordo, P., *Angew. Chem. Int. Ed.* **2013,** *52* (41), 10858-61.

12.   Zagdoun, A.; Casano, G.; Ouari, O.; Schwarzwälder, M.; Rossini, A. J.; Aussenac, F.; Yulikov, M.; Jeschke, G.; Copéret, C.; Lesage, A.; Tordo, P.; Emsley, L., *J. Am. Chem. Soc.* **2013,** *135* (34), 12790-7.

13.   Kubicki, D. J.; Casano, G.; Schwarzwälder, M.; Abel, S.; Sauvée, C.; Ganesan, K.; Yulikov, M.; Rossini, A. J.; Jeschke, G.; Copéret, C.; Lesage, A.; Tordo, P.; Ouari, O.; Emsley, L., *Chem. Sci.* **2016,** *7* (1), 550-8.

14.   Perras, F. A.; Reinig, R. R.; Slowing, I. I.; Sadow, A. D.; Pruski, M., *Phys. Chem. Chem. Phys.* **2016,** *18* (1), 65-9.

15.   Liao, W. C.; Ong, T. C.; Gajan, D.; Bernada, F.; Sauvée, C.; Yulikov, M.; Pucino, M.; Schowner, R.; Schwarzwälder, M.; Buchmeiser, M. R.; Jeschke, G.; Tordo, P.; Ouari, O.; Lesage, A.; Emsley, L.; Copéret, C., *Chem Sci* **2017,** *8* (1), 416-422.

16.   Kiesewetter, M. K.; Michaelis, V. K.; Walish, J. J.; Griffin, R. G.; Swager, T. M., *J Phys Chem B* **2014,** *118* (7), 1825-30.

17.   Sauvée, C.; Casano, G.; Abel, S.; Rockenbauer, A.; Akhmetzyanov, D.; Karoui, H.; Siri, D.; Aussenac, F.; Maas, W.; Weber, R. T.; Prisner, T.; Rosay, M.; Tordo, P.; Ouari, O., *Chem. - Eur. J.* **2016,** *22* (16), 5598-606.

9

18. Jagtap, A. P.; Geiger, M. A.; Stoppler, D.; Orwick-Rydmark, M.; Oschkinat, H.; Sigurdsson, S. T., *Chem. Commun.* **2016,** *52* (43), 7020-3.

19. Zagdoun, A.; Rossini, A. J.; Gajan, D.; Bourdolle, A.; Ouari, O.; Rosay, M.; Maas, W. E.; Tordo, P.; Lelli, M.; Emsley, L.; Lesage, A.; Coperet, C., *Chem. Commun.* **2012,** *48* (5), 654-6.

20. Kubicki, D. J.; Rossini, A. J.; Purea, A.; Zagdoun, A.; Ouari, O.; Tordo, P.; Engelke, F.; Lesage, A.; Emsley, L., *J. Am. Chem. Soc.* **2014,** *136* (44), 15711-8.

21. Thurber, K. R.; Tycko, R., *J. Chem. Phys.* **2012,** *137* (8), 084508.

22. Mance, D.; Gast, P.; Huber, M.; Baldus, M.; Ivanov, K. L., *J. Chem. Phys.* **2015,** *142*, 234201.

23. Mentink-Vigier, F.; Akbey, Ü.; Oschkinat, H.; Vega, S.; Feintuch, A., *J. Magn. Reson.* **2015,** *258*, 102-20.

24. Chaudhari, S. R.; Berruyer, P.; Gajan, D.; Reiter, C.; Engelke, F.; Silverio, D.; Copéret, C.; Lelli, M.; Lesage, A.; Emsley, L., *Phys. Chem. Chem. Phys.* **2016,** *18*, 10616-22.

25. Mentink-Vigier, F.; Akbey, Ü.; Hovav, Y.; Vega, S.; Oschkinat, H.; Feintuch, A., *J. Magn. Reson.* **2012,** *224*, 13-21.

26. Mentink-Vigier, F.; Paul, S.; Lee, D.; Feintuch, A.; Hediger, S.; Vega, S.; De Paëpe, G., *Phys. Chem. Chem. Phys.* **2015,** *17* (34), 21824-36.

27. Thurber, K. R.; Tycko, R., *J. Chem. Phys.* **2014,** *140* (18), 184201.

28. Lelli, M.; Chaudhari, S. R.; Gajan, D.; Casano, G.; Rossini, A. J.; Ouari, O.; Tordo, P.; Lesage, A.; Emsley, L., *J. Am. Chem. Soc.* **2015,** *137* (46), 14558-61.

29. Chaudhari, S. R.; Wisser, D.; Pinon, A. C.; Berruyer, P.; Gajan, D.; Tordo, P.; Ouari, O.; Reiter, C.; Engelke, F.; Copéret, C.; Lelli, M.; Lesage, A.; Emsley, L., *J. Am. Chem. Soc.* **2017,** *139* (31), 10609-12.

30. Hu, K. N.; Bajaj, V. S.; Rosay, M.; Griffin, R. G., *J. Chem. Phys.* **2007,** *126* (4), 044512.

31. Mathies, G.; Caporini, M. A.; Michaelis, V. K.; Liu, Y.; Hu, K. N.; Mance, D.; Zweier, J. L.; Rosay, M.; Baldus, M.; Griffin, R. G., *Angew. Chem. Int. Ed.* **2015,** *54* (40), 11770-4.

32. Mentink-Vigier, F.; Mathies, G.; Liu, Y.; Barra, A.-L.; Caporini, M.; Lee, D.; Hediger, S.; Griffin, R. G.; De Paëpe, G., *Chem. Sci.* **2017,** *8*, 8150-63.

33. Bothe, S.; Nowag, J.; Klimavičius, V.; Hoffmann, M. M.; Troitskaya, T. I.; Amosov, E. V.; Tormyshev, V. M.; Kirilyuk, I.; Taratayko, A.; Kuzhelev, A. A.; Parkhomenko, D.; Bagryanskaya, E. G.; Gutmann, T.; Buntkowsky, G., *J. Phys. Chem. C* **2018,** *122* (21), 11422-32.

34. Zhai, W.; Feng, Y.; Liu, H.; Rockenbauer, A.; Mance, D.; Li, S.; Song, Y.; Baldus, M.; Liu, Y., *Chem. Sci.* **2018,** *9*, 4381-91.

35. Lumata, L.; Kovacs, Z.; Sherry, A. D.; Malloy, C.; Hill, S.; van Tol, J.; Yu, L.; Song, L.; Merritt, M. E., *Phys. Chem. Chem. Phys.* **2013,** *15* (24), 9800-7.

36. Michaelis, V. K.; Smith, A. A.; Corzilius, B.; Haze, O.; Swager, T. M.; Griffin, R. G., *J. Am. Chem. Soc.* **2013,** *135* (8), 2935-8.

37. Haze, O.; Corzilius, B.; Smith, A. A.; Griffin, R. G.; Swager, T. M., *J. Am. Chem. Soc.* **2012,** *134*, 14287-90.

38. Dane, E. L.; Maly, T.; Debelouchina, G. T.; Griffin, R. G.; Swager, T. M., *Org. Let.* **2009,** *11* (9), 1871-4.

39. Pinto, L. F.; Marin-Montesinos, I.; Lloveras, V.; Munoz-Gomez, J. L.; Pons, M.; Veciana, J.; Vidal-Gancedo, J., *Chem. Commun.* **2017,** *53* (26), 3757-60.

40. Thurber, K.; Tycko, R., *J. Magn. Reson.* **2009,** *196*, 84-87.

41. Bendall, R. M.; Gordon, R. E., *J. Magn. Reson.* **1983,** *53*, 365-85.

42. Cory, D. G., Ritchey, W. M., *J. Magn. Reson.* **1988,** *80*, 128-32.

43. Bodenhausen, G.; Freeman, R.; Turner, D. L., *J. Magn. Reson.* **1977,** *27*, 511-14.

44. Lesage, A.; Lelli, M.; Gajan, D.; Caporini, M. A.; Vitzthum, V.; Miéville, P.; Alauzun, J.; Roussey, A.; Thieuleux, C.; Mehdi, A.; Bodenhausen, G.; Copéret, C.; Emsley, L., *J. Am. Chem. Soc.* **2010,** *132*, 15459-61.

45. Fung, B. M.; Khitrin, A. K.; Ermolaev, K., *J. Magn. Reson.* **2000,** *142* (1), 97-101.

46. Lesage, A.; Bardet, M.; Emsley, L., *J. Am. Chem. Soc.* **1999,** *121* (47), 10987-10993.

47. Stoll, S.; Schweiger, A., *J. Magn. Reson.* **2006,** *178*, 42-55.

48. Song, C.; Hu, K. N.; Joo, C. G.; Swager, T. M.; Griffin, R. G., *J. Am. Chem. Soc.* **2006,** *128*, 11385-90.

49. Snipes, W.; Cupp, J.; Cohn, G.; Keith, A., *Biophys. J.* **1974,** *14* (1), 20-32.

50. Kobayashi, T.; Perras, F. A.; Chaudhary, U.; Slowing, I. I.; Huang, W.; Sadow, A. D.; Pruski, M., *Solid State Nucl. Magn. Reson.* **2017,** *87*, 38-44.

51. Perras, F. A.; Wang, L.-L.; Manzano, J. S.; Chaudhary, U.; Opembe, N. N.; Johnson, D. D.; Slowing, I. I.; Pruski, M., *Curr. Opin. Colloid Interface Sci.* **2018,** *33*, 9-18.

52. Liao, W.-C.; Ghaffari, B.; Gordon, C. P.; Xu, J.; Copéret, C., *Curr. Opin. Colloid Interface Sci.* **2018,** *33*, 63-71.

53. Nanni, E. A.; Barnes, A. B.; Matsuki, Y.; Woskov, P. P.; Corzilius, B.; Griffin, R. G.; Temkin, R. J., *J. Magn. Reson.* **2011,** *210* (1), 16-23.

54. Perras, F. A.; Kobayashi, T.; Pruski, M., *J. Magn. Reson.* **2016,** *264*, 125-30.

55. Björgvinsdottir, S.; Walder, B. J.; Pinon, A. C.; Yarava, J. R.; Emsley, L., *J. Magn. Reson.* **2018,** *288*, 69-75.

56. Rossini, A. J.; Zagdoun, A.; Lelli, M.; Gajan, D.; Rascón, F.; Rosay, M.; Maas, W. E.; Copéret, C.; Lesage, A.; Emsley, L., *Chem. Sci.* **2012,** *3* (1), 108-15.

57. Corzilius, B.; Andreas, L. B.; Smith, A. A.; Ni, Q. Z.; Griffin, R. G., *J. Magn. Reson.* **2014,** *240*, 113-23.

58. Vitzthum, V.; Mieville, P.; Carnevale, D.; Caporini, M. A.; Gajan, D.; Copéret, C.; Lelli, M.; Zagdoun, A.; Rossini, A. J.; Lesage, A.; Emsley, L.; Bodenhausen, G., *Chem. Commun.* **2012,** *48* (14), 1988-90.

59. Valla, M.; Rossini, A. J.; Caillot, M.; Chizallet, C.; Raybaud, P.; Digne, M.; Chaumonnot, A.; Lesage, A.; Emsley, L.; van Bokhoven, J. A.; Copéret, C., *J. Am. Chem. Soc.* **2015,** *137* (33), 10710-19.

60. Mouat, A. R.; George, C.; Kobayashi, T.; Pruski, M.; van Duyne, R. P.; Marks, T. J.; Stair, P. C., *Angew. Chem. Int. Ed.* **2015,** *54* (45), 13346-51.

61. Kwak, J. H.; Hu, J.; Mei, D.; Yi, C.-W.; Kim, D. H.; Peden, C. H.; Allard, L. F.; Szanyi, J., *Science* **2009,** *325* (5948), 1670.

62. Kerber, R. N.; Kermagoret, A.; Callens, E.; Florian, P.; Massiot, D.; Lesage, A.; Copéret, C.; Delbecq, F.; Rozanska, X.; Sautet, P., *J. Am. Chem. Soc.* **2012,** *134* (15), 6767-75.

63. Wischert, R.; Florian, P.; Copéret, C.; Massiot, D.; Sautet, P., *J. Phys. Chem. C* **2014,** *118* (28), 15292-9.

64. Corma, A., *Chem. Rev.* **1995,** *95* (3), 559-614.

65. Busca, G., *Chem. Rev.* **2007,** *107* (11), 5366-5410.

66. Pérez-Ramírez, J.; Christensen, C. H.; Egeblad, K.; Christensen, C. H.; Groen, J. C., *Chem. Soc. Rev.* **2008,** *37* (11), 2530-2542.

67. Chizallet, C.; Raybaud, P., *Chem. Phys. Chem.* **2010,** *11* (1), 105-8.

10

1
2
3
4
5
6
7
8
9
10
11
12
13
14
15
16
17
18
19
20
21
22
23
24
25
26
27
28
29
30
31
32
33
34
35
36
37
38
39
40
41
42
43
44
45
46
47
48
49
50
51
52
53
54
55
56
57
58
59
60